

ORIGINAL RESEARCH

S100a8/9 (S100 Calcium Binding Protein a8/9) Promotes Cardiac Hypertrophy Via Upregulation of FGF23 (Fibroblast Growth Factor 23) in Mice

Yu-Pei Yuan, PhD*¹; Zhuo-Yu Shen, MS*¹; Teng Teng , MS; Si-Chi Xu, PhD; Chun-Yan Kong, PhD; Xiao-Feng Zeng, BSc; Marion A. Hofmann Bowman , MD, PhD; Ling Yan , MD, PhD

BACKGROUND: S100a8/9 (S100 calcium binding protein a8/9) belongs to the S100 family and has gained a lot of interest as a critical regulator of inflammatory response. Our previous study found that S100a8/9 homolog promoted aortic valve sclerosis in mice with chronic kidney disease. However, the role of S100a8/9 in pressure overload-induced cardiac hypertrophy remains unclear. The present study was to explore the role of S100a8/9 in cardiac hypertrophy.

METHODS AND RESULTS: Cardiomyocyte-specific S100a9 loss or gain of function was achieved using an adeno-associated virus system, and the model of cardiac hypertrophy was established by aortic banding-induced pressure overload. The results indicate that S100a8/9 expression was increased in response to pressure overload. S100a9 deficiency alleviated pressure overload-induced hypertrophic response, whereas S100a9 overexpression accelerated cardiac hypertrophy. S100a9-overexpressed mice showed increased FGF23 (fibroblast growth factor 23) expression in the hearts after exposure to pressure overload, which activated calcineurin/NFAT (nuclear factor of activated T cells) signaling in cardiac myocytes and thus promoted hypertrophic response. A specific antibody that blocks FGFR4 (FGF receptor 4) largely abolished the prohypertrophic response of S100a9 in mice.

CONCLUSIONS: In conclusion, S100a8/9 promoted the development of cardiac hypertrophy in mice. Targeting S100a8/9 may be a promising therapeutic approach to treat cardiac hypertrophy.

Key Words: cardiac hypertrophy ■ fibroblast growth factor 23 ■ fibroblast growth factor receptor 4 ■ S100a8/9 protein ■ therapeutic target

Cardiac hypertrophy is characterized by cardiomyocyte hypertrophy, fibroblast proliferation, extracellular matrix accumulation, and inflammatory cell infiltration, leading to congestive heart failure and high rates of mortality and morbidity.¹ As the key pathophysiologic process of heart failure, although cardiac hypertrophy has been extensively studied, the underlying precise mechanisms are incompletely understood.

Nevertheless, accumulating evidence suggests that calcineurin/NFAT (nuclear factor of activated T cells) pathway plays a pivotal role.^{2,3}

Activation of calcineurin/NFAT pathway has been reported in varied cardiac hypertrophy models.^{3–5} Notably, sustained activation of calcineurin in heart is sufficient to induce cardiac hypertrophy that progresses rapidly to dilated hypertrophy and heart failure.^{6,7} On

Correspondence to: Ling Yan, MD, PhD, Department of Cardiology, Renmin Hospital of Wuhan University, Hubei Key Laboratory of Metabolic and Chronic Diseases, 430060 Wuhan, PR China. Email: lingyan@whu.edu.cn

*Y.-P. Yuan and Z.-Y. Shen contributed equally.

This article was sent to Ferhaan Ahmad, MD, PhD, Senior Associate Editor, for review by expert referees, editorial decision, and final disposition.

Supplemental Material is available at <https://www.ahajournals.org/doi/suppl/10.1161/JAHA.122.028006>

For Sources of Funding and Disclosures, see page 13.

© 2024 The Authors. Published on behalf of the American Heart Association, Inc., by Wiley. This is an open access article under the terms of the [Creative Commons Attribution-NonCommercial-NoDerivs](https://creativecommons.org/licenses/by-nc-nd/4.0/) License, which permits use and distribution in any medium, provided the original work is properly cited, the use is non-commercial and no modifications or adaptations are made.

JAHA is available at: www.ahajournals.org/journal/jaha

RESEARCH PERSPECTIVE

What Is New?

- This study reports an exacerbated role of S100a8/9 (S100 calcium binding protein a8/9) in pressure overload-induced cardiac hypertrophy and dysfunction via increased expression of FGF23 (fibroblast growth factor 23).

What Question Should Be Addressed Next?

- In the next phase, we will construct S100a gene knockout mice to further validate the role of the S100a gene in the underlying mechanisms of myocardial hypertrophy.

Nonstandard Abbreviations and Acronyms

FGF23	fibroblast growth factor 23
FGFR4	FGF receptor 4
RCAN1	regulator of calcineurin 1
S100a8/9	S100 calcium binding protein a8/9

activation by calcium, calcineurin binds and dephosphorylates NFAT, resulting in the translocation of NFAT to the nucleus and activation of hypertrophy-related genes.⁷ Conversely, inhibition of calcineurin/NFAT attenuates the development process of cardiac hypertrophy.⁸ These studies suggest the calcineurin/NFAT pathway contributes to hypertrophic progression, and the inhibition of this signaling pathway could help in developing efficacious interventions for the treatment of cardiac hypertrophy.

S100a8/9 (S100 calcium binding protein a8 and a9) are members of the S100 protein family, which is secreted by several inflammatory cells.⁹ High serum level of S100a8/9 has been identified as a risk factor of cardiovascular death.¹⁰ Knockdown of S100a8/9 resulted in reduced apoptosis, suppressed cardiac hypertrophy, and improved cardiac function in mice with myocardial infarction.¹¹ S100a8/9 were also closely involved into the process of doxorubicin-induced cardiotoxicity,¹² coxsackievirus B3-induced myocarditis,¹³ and endotoxin-induced cardiac dysfunction.¹⁴ Moreover, our previous study revealed that elevated levels of S100a12 (human homolog of S100a8/9) in the serum of mice with chronic kidney disease promoted pathological cardiac remodeling.¹⁵ These findings raised the possibility that S100a8/9 would promote pressure overload-induced cardiac hypertrophy. In the present study, we report our investigation into the

specific effects of S100a8/9 on overload-induced cardiac hypertrophy.

The data that support the findings of this study are available from the corresponding author upon reasonable request.

METHODS

Reagents

The following primary antibodies were purchased from Cell Signaling Technology (Boston, MA): S100a8 (1:1000), S100a9 (1:1000), PLC γ (phospholipase C- γ ; 1:1000), P-PLC γ (phospho-PLC γ ; 1:1000), calcineurin (1:1000), NFATc3 (1:1000), FGF23 (fibroblast growth factor 23; 1:1000), and GAPDH (1:1000). PCNA (proliferating cell nuclear antigen, 1:200) antibody was purchased from Santa Cruz Biotechnology (Dallas, TX). Adeno-associated virus (AAV9) carrying S100a9 or GFP (green fluorescent protein) used in our study was generated by Hanbio (Shanghai, China). Knockdown of S100a9 was carried out using AAV9 vectors carrying small hairpin RNAs (shRNAs) targeting S100a9, which were also generated by Hanbio. Scrambled shRNA was used as the control. The inhibitors, PD169316, SP600125, U0126, VIVIT, AKTi, CCT129957, and cyclosporin A were purchased from MedChemExpress (Wuhan, China).

Animals and Treatments

All animal experimental procedures were approved by the Guidelines for Animal Care and Use Committee of Renmin Hospital of Wuhan University, which is also in agreement with the *Guidelines for the Care and Use of Laboratory Animals* published by the United States National Institutes of Health (NIH Publication, revised 2011). Male C57BL/6 mice (8- to 10-week-old; body weight: 25.5 \pm 2g) were obtained from the Institute of Laboratory Animal Science, Chinese Academy of Medical Sciences (Beijing, China). These mice were allowed free access to food and drinking water. They were fed in a house in which the temperature (20–25 °C) and humidity (50% \pm 5%) were under strict control and the light was kept at a 12-hour light–dark cycle. To investigate the specific effects of S100a8/9, C57BL/6 mice were divided randomly into 4 groups: shRNA+sham, shS100a8/9+sham, shRNA+aortic banding (AB), and shS100a8/9+AB. To knock down the protein expression of S100a8/9 in hearts, each mouse was subjected to an injection of 2.5 \times 10¹¹ AAV9 vectors carrying shS100a9 or scrambled shRNA under the cTnT (cardiac troponin T) promoter at the day of AB surgery.^{16,17} The procedures of AB or sham surgery were described in our previous studies.^{18,19} Six weeks after AB surgery, all mice were anesthetized with 1.5% isoflurane, and echocardiographic measurements

were performed. After that, mice were euthanized and hearts were weighed and snap-frozen in liquid nitrogen for further detection. To overexpress S100a9, mice were given a single injection of AAV9 carrying S100a9 or GFP under the cTnT promoter at a dose of 2×10^{11} viral genome particles/mouse via the tail vein.²⁰ All mice were divided randomly into 4 groups: GFP+sham, S100a9+sham, GFP+AB, and S100a9+AB. Three weeks after injection, AB or sham surgery was performed. Three weeks after AB surgery, echocardiographic measurements were performed. After that, hearts were weighed and collected.

To ascertain whether FGF23 was responsible for enhanced hypertrophic response caused by S100a8/9, C57BL/6 mice were subjected to repeated intraperitoneal injections of anti-FGF receptor 4 (FGFR4) blocking antibody (human monoclonal, U3-11; U3Pharma) at 25 mg/kg per day every 3 days, with the first injection beginning after AB surgery.²¹ At the end point of treatment, all the mice were anesthetized with 1.5% isoflurane, and echocardiographic measurements were performed. After that, hearts were weighed and snap-frozen in liquid nitrogen for further detection.

Echocardiography

After the mice were anesthetized by 1.5% isoflurane, transthoracic echocardiography was performed by a MyLab 30CV ultrasound (Esaote SpA, Genoa, Italy) with a 10-MHz linear array ultrasound transducer to obtain M-mode images at the papillary muscle level for measurement of wall thickness, chamber dimensions, and cardiac function.

Morphometric Analyses

Obtained hearts were arrested in diastole in 10% KCl and then fixed with 4% formaldehyde overnight. After that, hearts were embedded in paraffin, sectioned into 5- μ m slices, and stained with hematoxylin and eosin to count cardiomyocytes area and stained with picosirius red to measure cardiac fibrosis. The cross-sectional area and fibrosis area (average collagen volume) were counted by a digital analysis system (Image-Pro Plus 6.0, Media Cybernetics, Bethesda, MD). For detection of cardiomyocytes area, more than 50 cells per slide were determined.

After being stained with picosirius red, slices were photographed under light microscopy and then analyzed by aforementioned image analysis system. The collagen volume fraction was determined by Image J software as an index of cardiac fibrosis area. Five visual fields without small coronary arteries were randomly examined in each slice. For each photograph, red color (collagen) area and total tissue area were measured. Subsequently, the percentage of the collagen volume fraction were calculated according to the

formula: collagen volume fraction=collagen area/total tissue area $\times 100\%$. Five collagen volume fractions were scored for each slice, and the mean was calculated.

GFP Fluorescence Examination

At the end point of treatment, hearts were harvested, embedded in tissue-freezing medium (Triangle Biomedical Sciences), frozen in liquid nitrogen for 10 minutes, and placed at -80°C overnight. These heart samples were then frozen in Tissue-Tek O.C.T. compound (Sakura Fintek, USA) and sectioned on a microtome. Frozen sections at 15- μ m in thickness were prepared with a Leica CM1850 cryostat for fluorescence microscopy.

Western Blot and Quantitative Real-Time Polymerase Chain Reaction

RIPA lysis buffer (Invitrogen, Carlsbad, CA) was used to isolate total protein from the frozen heart tissues or iced cell lysates. Nuclear protein extracts were isolated using a commercial kit. Then, proteins were separated by 10% SDS-PAGE and transferred onto polyvinylidene fluoride membranes (cat. number IPFL00010; EMD Millipore, Billerica, MA). Next, the membranes were blocked with 5% nonfat milk at room temperature and incubated with the primary antibodies at 4°C overnight. After incubating with the secondary antibodies at 37°C for 1 hour, the polyvinylidene fluoride membranes were scanned by the ChemiDoc XRS+ system and analyzed using an Image Lab software (Bio-Rad Laboratories, Inc.). Total RNA was isolated and reverse-transcribed to cDNA by Transcriptor First Strand cDNA Synthesis Kit (Roche, Basel, Switzerland, 04896866001). The quantification of real time polymerase chain reaction was performed using the LightCycler 480 SYBR Green Master Mix (cat. Number 04896866001; Roche). The protein levels were normalized to GAPDH and nuclear proteins were normalized to PCNA. Phosphorylation was normalized to the matched total protein. The mRNA data were normalized to *Gapdh*.

Cell Culture and Treatment

Neonatal rat cardiomyocytes (NRCMs) were prepared as previously described.^{18,20} Bromodeoxyuridine (BrdU, 0.1 mmol/L) was used to inhibit cardiac fibroblast proliferation in NRCMs. NRCMs were seeded onto 6-well plates and cultured in DMEM/F12 (GIBCO) containing 10% FBS (GIBCO) for 48 hours. Then, the culture medium was replaced with serum free DMEM/F12 for 16 hours to synchronize the cells before the experiment. To induce cardiomyocyte hypertrophy, NRCMs were treated with phenylephrine (50 μ mol/L) for 48 hours. We treated the cells with phenylephrine because pressure overload-induced

cardiac hypertrophy was at least partly dependent on the activation of α 1-adrenergic receptor, and this α 1-adrenergic activator could induce cardiomyocyte hypertrophic growth in vitro.²⁰ To determine whether S100a8/9 affects cardiomyocyte hypertrophy, NRCMs were stimulated by recombinant S100a8/9 for 24 hours in the presence of phenylephrine incubation. rS100a8 and rS100a9 proteins were purchased from Prospec (Rehovot, Israel). Then, we knocked down the protein expression of S100a9 in NRCMs using siS100a9. NRCMs were preincubated with adenoviruses carrying siS100a9 or siRNA for 4 hours and then subjected to phenylephrine treatment for 48 hours. siS100a9 and siRNA were generated by RiboBio (RiboBio Co., Ltd, Guangzhou, China). To investigate the precise molecular mechanism of S100a8/9 in cardiac hypertrophy, NRCMs were simultaneously treated with a specific inhibitor of p38 MAP kinase (PD169316, 10 μ mol/L), a specific inhibitor of JNK (SP600125, 10 μ mol/L), a specific inhibitor of ERK (U0126, 10 μ mol/L), a specific inhibitor of NF- κ B (nuclear factor- κ B; BMS-345541, 10 μ mol/L), a specific inhibitor of calcineurin (cyclosporin A, 1 μ mol/L), a specific inhibitor of NFAT (VIVIT, 1 μ mol/L), a specific inhibitor of PLC- γ (CCT129957, 1 μ mol/L) and an AKT inhibitor (AKTi, 1 μ mol/L), respectively. To investigate whether FGFR4 is responsible for the effects of S100a8/9 on hypertrophic response, these recombinant S100a8/9-incubated NRCMs were pretreated with FGFR4 blocking antibody (10 mg/mL) for 24 hours. Immunoglobulin G was used in the control group. For reactive oxygen species (ROS) scavenging, NRCMs were pretreated with NAC (10 mmol/L) or vehicle for 30 minutes before phenylephrine (50 μ mol/L) stimulation.

Immunofluorescence

The immunofluorescence was performed as previously described. Briefly, the cells on coverslips were fixed with 4% paraformaldehyde, permeabilized in 0.5% Triton X-100 and then incubated with α -actinin (1: 100) overnight at 4 °C followed by incubation with Alexa 568-conjugated goat-anti mouse antibody (1:200) for 60 minutes at 37 °C. To visualize nuclei, the slides were mounted with DAPI. Immunofluorescence images were taken on the OLYMPUS DX51 fluorescence microscope (Tokyo, Japan). Images were quantified by Image-Pro Plus 6.0.

Measurement of Superoxide Dismutase Activities and ROS Production

The activities of total superoxide dismutase were assessed spectrophotometrically in NRCMs culture supernatants using commercial assay kits (Nanjing Jiancheng Bioengineering Institute, China) according to the provided instructions.

To measure the level of ROS production, NRCMs were incubated with DCFH-DA (5 μ mol/L) at 37 °C for 2 hours and washed. Fluorescence was observed under an OLYMPUS IX53 fluorescence microscope. ROS was also quantified using electron spin resonance (ESR) spectroscopy (Bruker, Karlsruhe, Germany) with 5,5-dimethyl-1-pyrroline N-oxide (DMPO, Sigma) at a final concentration of 100 mmol/L as described previously.

Measurement of Calcineurin Activity

The calcineurin activity in tissues was determined by the Calcineurin Cellular Assay Kit PLUS-AK-816 (BioMol) according to the manufacturer's instructions. The kit was a product in the BIOMOL GREEN QuantiZyme Assay system and was a complete colorimetric assay kit for measuring cellular calcineurin phosphatase activity. Extracts of tissues were prepared, and calcineurin activity was measured as the dephosphorylation rate of a synthetic phosphopeptide substrate (R11 peptide). The amount of PO₄³⁻ released was determined colorimetrically with the BIOMOL GREEN reagent.

NFAT-Luciferase Reporter Mice and NFAT-Luciferase Activities

To confirm NFAT activation, NFAT-luciferase (NFAT-Luc) transgenic reporter mice (Stock No. 000465) aged 8 to 12 weeks were used from Jackson Laboratory (USA). These mice were fed in the same condition with C57 as described. To investigate the transcription level NFAT suffering different stimulations, each NFAT-Luc mouse was infected with shRNA or shS100a9 or GFP or S100a9. Four weeks after injection, AB or sham surgery was performed.

Heart tissue homogenates were prepared in Promega reporter lysis buffer using a Qiagen TissueLyser. Luciferase activity was measured by adding 20 μ L cell lysate to 100 μ L of freshly prepared CycLuc1 (AOBIOUS, catalog no. AOB 1117) luciferin substrate using a Promega GloMax luminometer. Luciferase activity was expressed as relative light units per milligram of protein.

Measurement of the Concentration of Fibroblast Growth Factor 23

The concentration of FGF23 was assessed spectrophotometrically in the fresh heart samples and cell culture supernatants using commercial assay kits (BIOESN, China) according to the provided instructions.

Statistical Analysis

Data in our study were presented as mean \pm SEM, and 1-way ANOVA were carried out to compare the difference among 3 or more groups followed by post hoc

Tukey test. Comparison between 2 groups was performed using an unpaired Student's *t* test. $P < 0.05$ was considered to be significant.

RESULTS

S100a8/9 Was Upregulated During the Hypertrophic Response

As shown in Figure 1A and 1B, S100a8/9 mRNA increased in mouse hearts 3 days after the onset of pressure overload, reaching the peak at 2 weeks. Western blot results suggested that S100a8/9 protein expression was also increased in the hearts of mice after 6-week AB surgery (Figure 1C). These data indicated that S100a8/9 may be implicated in the development of cardiac hypertrophy.

S100a8/9 Deficiency Attenuated Pressure Overload-Induced Cardiac Hypertrophy and Fibrosis in Mice

To determine whether S100a8/9 played a critical role in the development of cardiac hypertrophy, we used AAV9 to knock down S100a9 in the heart. As indicated

in Figure S1A, this AAV9 infection resulted in strong expression of GFP in the hearts, and the expression of GFP was not in a patchy pattern. AAV-shS100a9 infection resulted in the depletion of S100a8 and S100a9 (Figure S1B). The loss of S100a8 after S100a9 knockdown might be due to a greater turnover of isolated S100a8 in the absence of its binding partner S100a9.^{22,23} In response to pressure overload, mice exhibited an obvious hypertrophic phenotype, as indicated by the increased ratios of heart weight to body weight and heart weight to tibia length, cross-sectional area, and fibrotic area (Figure 2A through 2E). And these hypertrophic alterations were largely prevented by S100a9 loss of function in mice (Figure 2A through 2E). S100a9 deficiency decreased left ventricular internal diameter at end-diastole and interventricular septal thickness at diastole but increased ejection fraction in mice with hypertrophy caused by pressure overload (Figure 2F through 2H). Polymerase chain reaction analysis further determined the inhibitory effects on hypertrophic and fibrotic markers in S100a9-deficient hearts after exposure to pressure overload, as confirmed by the decreased ANP (atrial natriuretic peptide), BNP (brain natriuretic peptide), β -MHC (β -myosin heavy chain), α -MHC (alpha myosin heavy chain),

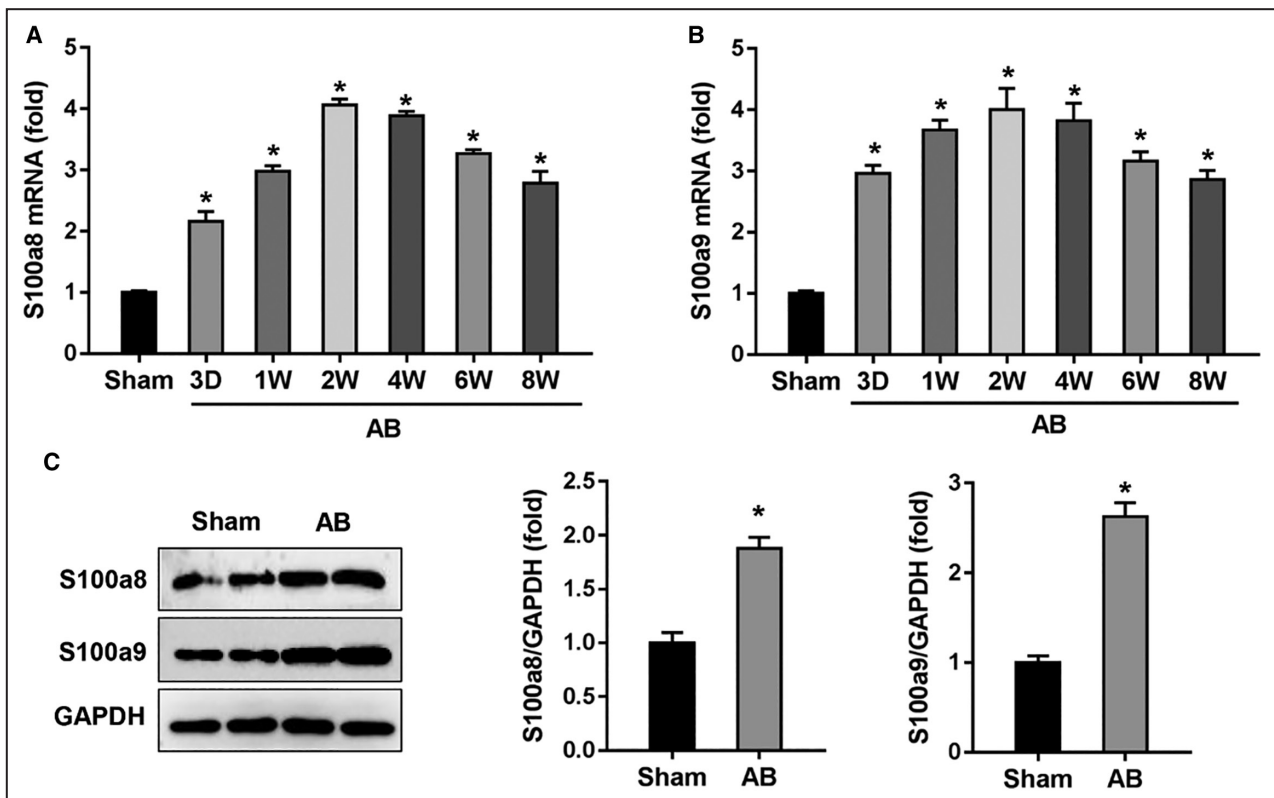


Figure 1. S100a8/9 was increased during the hypertrophic response.

A and **B**, The mRNA levels of S100a8 and S100a9 in Sham and aortic banding hearts ($n = 5$). **C**, Six weeks after AB surgery, Western blot analysis, and quantitative results of S100a8 and S100a9 ($n = 6$). Values represent the mean \pm SEM. * $P < 0.05$ vs Sham group. AB indicates aortic banding; and S100a8/9, S100 calcium binding protein a8/9.

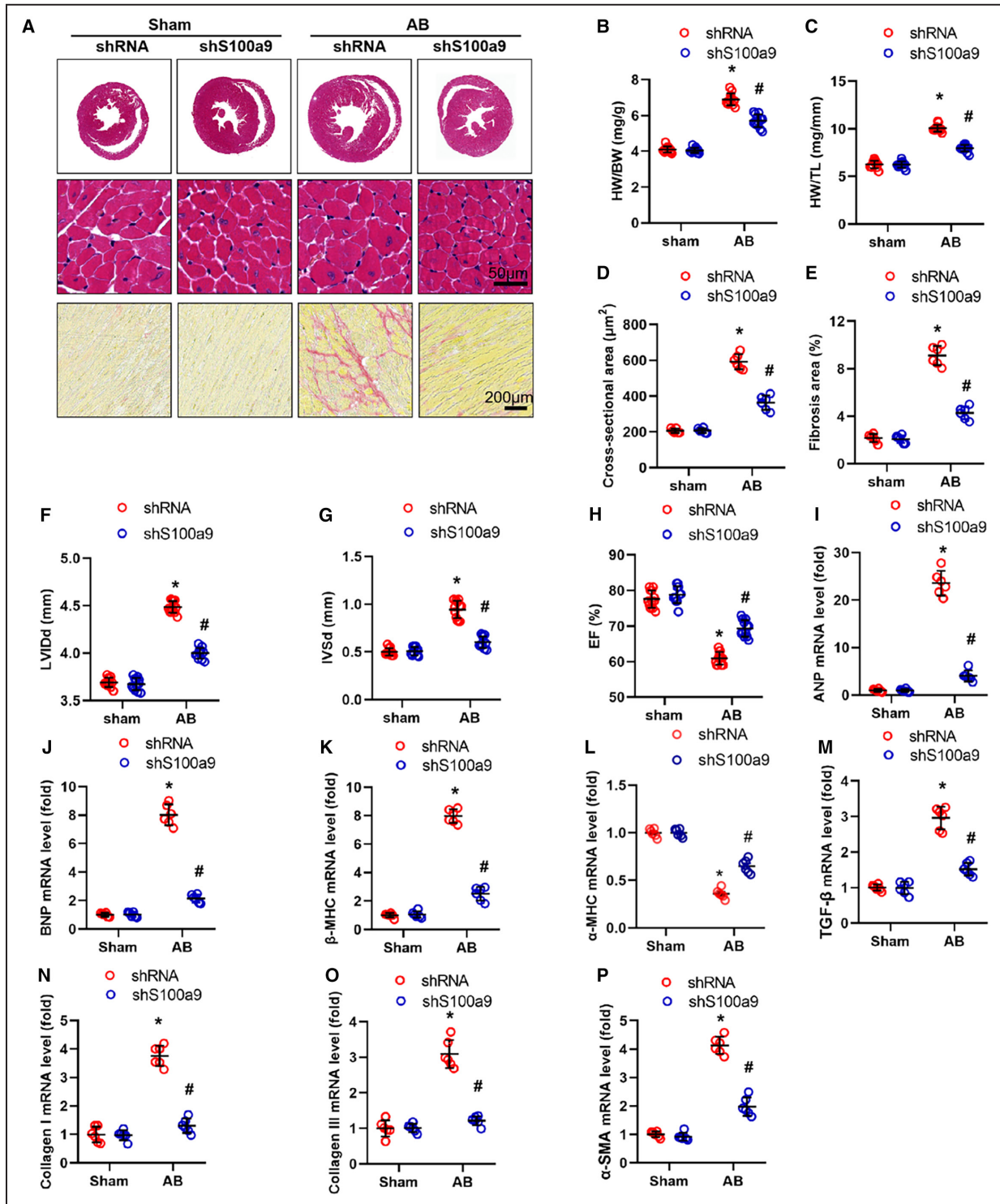


Figure 2. S100a8/9 deficiency attenuated pressure overload-induced cardiac hypertrophy and fibrosis in mice.

A, Six weeks after AB surgery, hematoxylin–eosin and picrosirius red staining of hearts with or without the infection of AAV9-shS100a9 (n=6). **B** and **C**, Statistical results of the HW/BW and HW/TL of 4 groups (n=12). **D**, Cross-sectional areas of myocytes (n=6). **E**, Statistical results of the fibrosis areas (n=6). **F** through **H**, LVIDd, IVSd, and EF of mice after AB surgery (n=12). **I–L**, mRNA levels of hypertrophy-related genes (n=6). **M** through **P**, The mRNA levels of fibrosis-related genes (n=6). Values represent the mean±SEM. **P*<0.05 vs Sham+shRNA, #*P*<0.05 vs AB+shRNA. AB indicates aortic banding; α-MHC, α-myosin heavy chain; α-SMA, α-smooth muscle actin; ANP, atrial natriuretic peptide; β-MHC, β-myosin heavy chain; BNP, B-type natriuretic peptide; BW, body weight; EF, ejection fraction; HW, heart weight; IVSd, interventricular septal thickness at diastole; LVIDd, left ventricular internal diastolic diameter; S100a8/9, S100 calcium binding protein a8/9; TGF-β, transforming growth factor β; and TL, tibia length.

TGF- β (transforming growth factor- β), Col I (collagen type I), Col III (collagen type III) and α -SMA (α -smooth muscle actin) (Figure 2I through 2P). Taken together, the present data indicate that S100a9 loss of function attenuates pressure overload-caused cardiac hypertrophy and fibrosis in mice, thus improving cardiac function in mice.

Overexpression of S100a9 in the Hearts Promoted Pressure Overload-Induced Cardiac Hypertrophy

Next, we overexpressed S100a9 in the hearts with AAV9 system. As indicated in Figure S1C, S100a9 and S100a8 protein levels were increased in the hearts of mice infected with AAV-S100a9. Pressure overload induced pathological hypertrophy in mice infected with AAV9 carrying GFP, as indicated by the increased heart weight to body weight and heart weight to tibia length ratios compared with the Sham group. These hypertrophic changes were further exacerbated by the expression of S100a9 in the hearts (Figure 3A through 3C). A larger cross-sectional area and more severe fibrosis were observed in S100a9-overexpressed mice when compared with those in the control groups (Figure 3D and 3E). Moreover, pressure overload-induced chamber dilation (left ventricular internal diameter at end-diastole) and systolic function impairment (ejection fraction) were more pronounced in S100a9-overexpressed mice than those in the control groups (Figure 3F through 3H). Detection of mRNA levels of several hypertrophic markers (ANP, BNP, β -MHC, and α -MHC) and fibrotic markers (TGF- β , Col I, Col III, and α -SMA) in S100a9-overexpressed mice after pressure overload further confirm the prohypertrophic role of S100a8/9 in vivo (Figure 3I through 3P). These data suggested that S100a8/9 promotes pressure overload-induced cardiac hypertrophy and fibrosis in mice.

S100a8/9 Promoted PE-Induced Hypertrophy of Cardiomyocytes In Vitro

Next, we used the model of PE-induced hypertrophy of cardiomyocytes to further decipher the prohypertrophic role of S100a8/9 in vitro. NRCMs were treated with recombinant S100a8/9 in the presence or absence of PE. Recombinant S100a8/9 aggravated PE-induced cardiomyocytes hypertrophy, as suggested by increased cell area and hypertrophic markers (ANP and β -MHC) (Figure 4A and 4B). We got similarity responses when transfecting an S100a9 expression plasmid into NRCMs (Figure S2A through S2C). Subsequently, we knocked down S100a9 with siRNA, and found that S100a8/9 deficiency resulted in a decrease in the hypertrophic phenotype in response to PE stimuli, as reflected by the decreased

cell area and hypertrophic markers (ANP and β -MHC) (Figure S2D; Figure 4C and 4D).

S100a8/9 Activated Calcineurin/NFAT Signaling Pathway During Phenylephrine-Induced Hypertrophy of Cardiomyocytes In Vitro

To study which signaling pathway was responsible for the hypertrophic effect of S100a8/9, NRCMs were treated with several inhibitors of hypertrophy-related kinases. We found that the prohypertrophic effects of S100a8/9 was blocked by cyclosporin A (an inhibitor of calcineurin), VIVIT (an inhibitor of NFAT), or CCT129957 (an inhibitor of PLC γ), but not PD169316 (an inhibitor of p38), SP600125 (an inhibitor of JNK), U0126 (an inhibitor of ERK), BMS-345541 (an inhibitor of NF- κ B), and an AKT inhibitor (Figure 5A and 5B). To determine if S100a8/9 could activate calcineurin/NFAT signaling pathway, we detected calcineurin activity in the hearts following pressure overload, and found that AB-induced calcineurin activity was enhanced by S100a9 overexpression but was attenuated by S100a9 knockdown (Figure 5C and 5D). Consistent with these findings, we also found that NFAT transcriptional activity was enhanced by S100a9 overexpression, but was attenuated by S100a9 knockdown (Figure 5E and 5F). Next, we detected the expression of RCAN1 (regulator of calcineurin 1), which was an NFAT target gene.²⁴ Elevated RCAN1 mRNA level was further enhanced by S100a9 gain of function but decreased by S100a9 loss of function in mice (Figure 5G and 5H). To further confirm the alterations of PLC γ and calcineurin/NFAT signaling pathway, we detected the protein expression of PLC γ and calcineurin/NFAT. S100a9 deficiency significantly decreased phosphorylated PLC γ levels without changing overall PLC γ expression in hypertrophic hearts (Figure 5I). The increased calcineurin protein expression and nuclear NFATc3 accumulation in response to pressure overload were also decreased by S100a9 deficiency (Figure 5I).

Mice With S100a9 Overexpression Exhibited Increased Cardiac Expression of FGF23

Our previous study revealed that global overexpression of human homolog of S100a8/9 in the mice with chronic kidney disease promoted pathological cardiac remodeling.¹⁵ This mouse line had an increased cardiac expression of FGF23.¹⁵ FGF23 induced binding of FGFR4 to PLC γ , thus activating calcineurin/NFAT signaling during cardiac hypertrophy.²¹ Therefore, we verified the hypothesis that the activation of PLC γ /calcineurin/NFAT signaling after hypertrophic stimuli triggers was dependent on the upregulation of FGF23. FGF23 mRNA and protein were

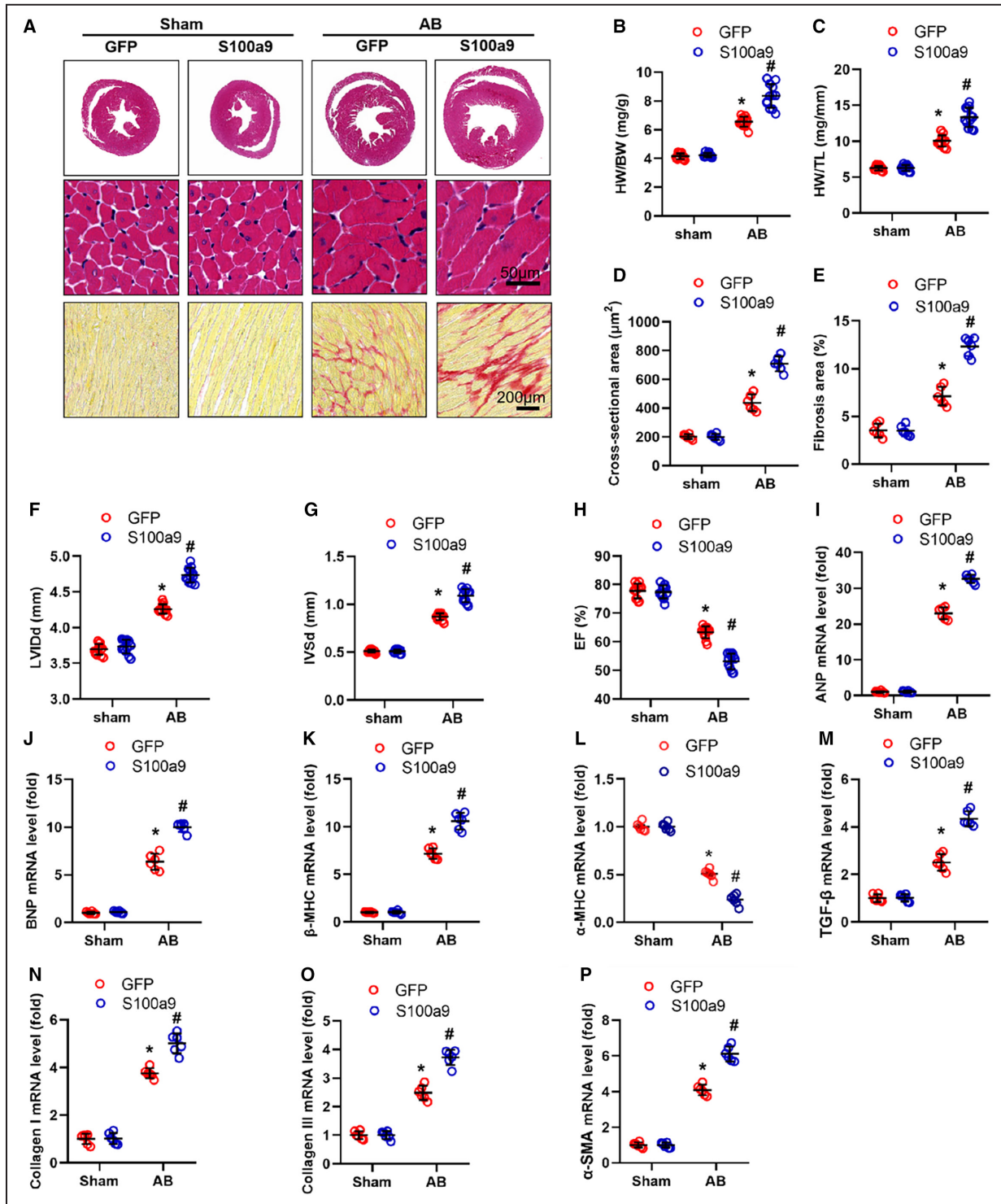


Figure 3. Overexpression of S100a9 in the hearts promoted pressure overload-induced cardiac hypertrophy.

A, Six weeks after AB surgery, hematoxylin–eosin and picrosirius red staining of hearts with or without the infection of AAV9-S100a9 (n=6). **B** and **C**, Statistical results of the HW/BW and HW/TL of 4 groups (n=12). **D**, The cross-sectional areas of myocytes (n=6). **E**, Statistical results of the fibrosis areas (n=6). **F** through **H**, LVIDd, IVSd, and EF of mice after AB surgery (n=12). **I** through **L**, mRNA levels of hypertrophy-related genes (n=6). **M** through **P**, mRNA levels of fibrosis-related genes (n=6). Values represent the mean±SEM. **P*<0.05 vs Sham+GFP, #*P*<0.05 vs AB+GFP. AAV9 indicates adeno-associated virus 9; AB, aortic banding; α-MHC, α-myosin heavy chain; α-SMA, α-smooth muscle actin; ANP, atrial natriuretic peptide; β-MHC, β-myosin heavy chain; BNP, B-type natriuretic peptide; BW, body weight; EF, ejection fraction; GFP, green fluorescent protein; HW, heart weight; IVSd, interventricular septal thickness at diastole; LVIDd, left ventricular internal diastolic diameter; S100a8/9, S100 calcium binding protein a8/9; TGF-β, transforming growth factor β; and TL, tibia length.

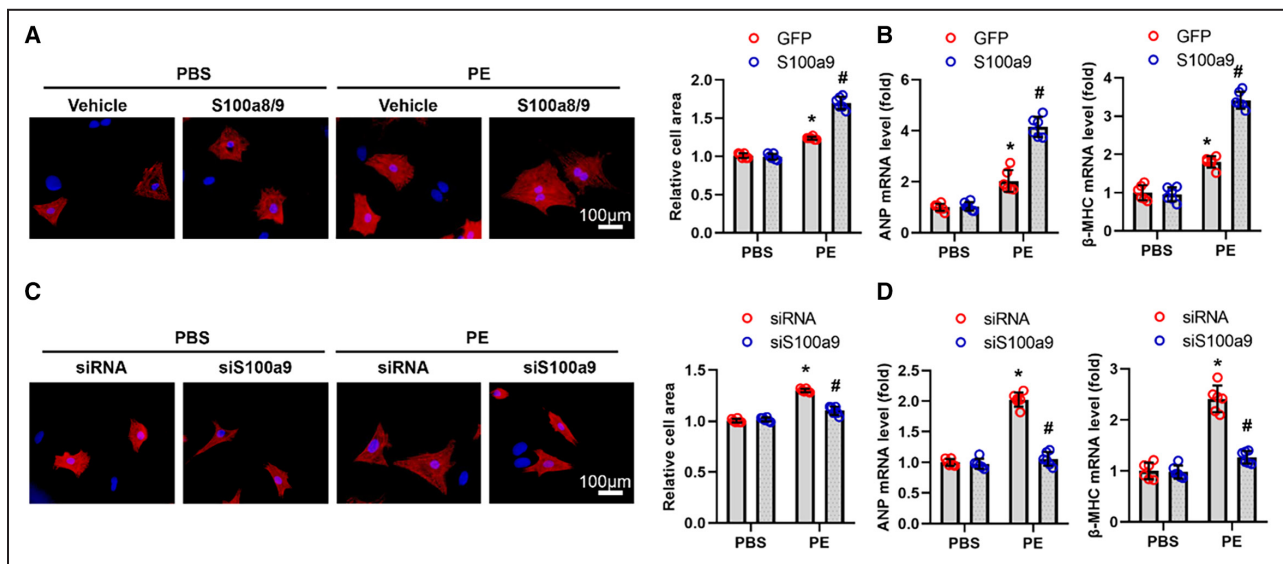


Figure 4. S100a8/9 promoted phenylephrine-induced hypertrophy of cardiomyocytes in vitro.

A, Representative α -actinin staining and cell area in neonatal rat cardiomyocytes (NRCMs) stimulated by recombinant S100a8/9 or not ($n=6$). **B**, mRNA levels of hypertrophic markers in NRCMs of indicated groups ($n=6$). **C**, Representative α -actinin staining and cell area in NRCMs infected with siS100a9 or not ($n=6$). **D**, mRNA levels of hypertrophic markers in NRCMs of indicated groups ($n=6$). Values represent the mean \pm SEM. For **A** and **B**, * $P<0.05$ vs PBS+Vehicle, # $P<0.05$ vs phenylephrine+S100a8/9. For **C** and **D**, * $P<0.05$ vs PBS+siRNA, # $P<0.05$ vs phenylephrine+siS100a9. ANP indicates atrial natriuretic peptide; β -MHC, β -myosin heavy chain; GFP, green fluorescent protein; and S100a8/9, S100 calcium binding protein a8/9.

largely increased in S100a9-overexpressed mice with pressure overload compared with AB mice infected with GFP (Figure 6A and 6B). There was no difference in FGF2 mRNA between the 2 groups (Figure 6A). AB-induced upregulation of FGF23 protein expression was also prevented by the deficiency of S100a9 (Figure 6C). We also detected FGF23 expression in PE-treated NRCMs and found that PE-induced FGF23 expression was limited by the deficiency of S100a9 but enhanced by the use of recombinant S100a8/9 (Figure 6D and 6E). FGF23 induced hypertrophic growth of cardiomyocytes through a direct FGFR4-dependent mechanism.²¹ NRCMs were pretreated with a FGFR4 blocking antibody. The data in our study demonstrated that this prohypertrophic effect of S100a8/9 was blocked by FGFR4 blocking antibody (Figure 6F through 6H). FGFR4 blocking antibody also abolished the enhancement of NFAT transcriptional activity caused by S100a8/9 treatment (Figure 6I).

FGFR4 Blocking Abolished the Prohypertrophic Effect of S100a8/9 Overexpression in Response to Pressure Overload

Next, we investigated whether FGF23-FGFR4 was responsible for the prohypertrophic effect of S100a8/9. S100a9-overexpressed mice were injected with an FGFR4 blocking antibody. S100a8/9 overexpression did not enhance pressure overload-induced hypertrophic response after FGFR4 blocking in mice. There

was no difference in hypertrophic response caused by pressure overload between AB+anti-FGFR4 and AB+S100a8/9+anti-FGFR4 groups, as reflected by the heart weight to body weight ratio, cross-sectional area, fibrotic area, and cardiac function (Figure 7A through 7F). The enhanced calcineurin-NFAT activity and RCAN1 expression in S100a9-overexpressed mice were also suppressed by the use of this FGFR4 blocking antibody (Figure 7G through 7I).

ROS Was Responsible for the Upregulation of FGF23 in S100a8/9-Treated Cells After Phenylephrine Treatment

We also found that S100a8/9 increased phenylephrine-induced ROS production and further decreased the total superoxide dismutase activity in phenylephrine-treated cells (Figure S3A and S3B). Next, we confirmed whether the upregulation of FGF23 in S100a8/9-treated cells was dependent on ROS production. We used a ROS scavenger, NAC, and found that NAC blocked the elevation of FGF23 and enhanced cell area of S100a8/9-treated cells (Figure S3C and S3D).

DISCUSSION

In the present study, we found that S100a8/9 was increased during pressure overload-induced cardiac remodeling. Cardiac-specific depletion of S100a9

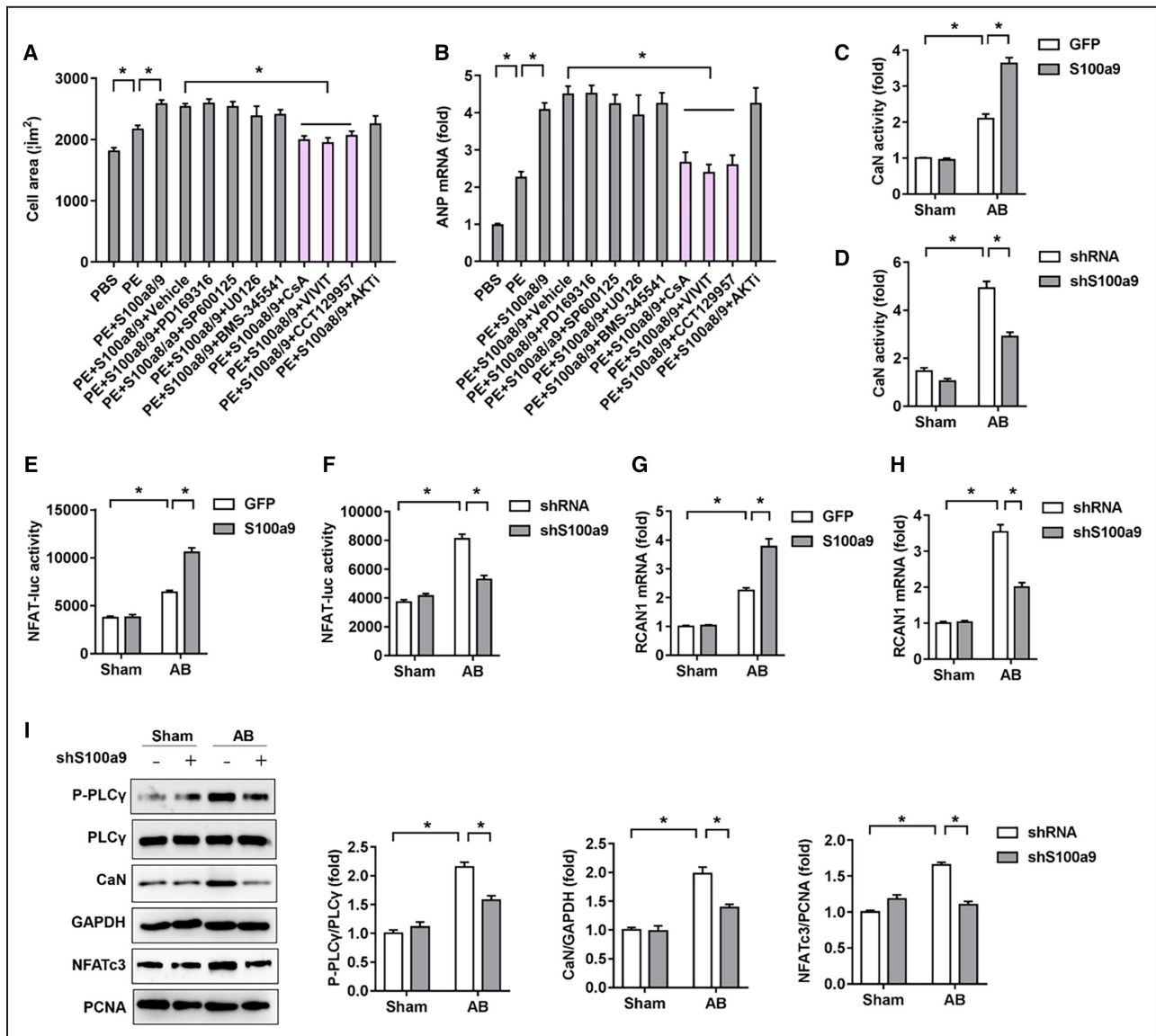


Figure 5. S100a8/9 activated calcineurin/NFAT signaling pathway during phenylephrine-induced hypertrophy of cardiomyocytes in vitro.

A, Cell areas of NRCMs treated with several inhibitors of hypertrophy-related kinases (n=5), cyclosporin A (an inhibitor of calcineurin), VIVIT (an inhibitor of NFAT), CCT129957 (an inhibitor of PLC γ), PD169316 (an inhibitor of p38), SP600125 (an inhibitor of JNK), U0126 (an inhibitor of ERK), BMS-345541 (an inhibitor of NF- κ B), and AKTi (an inhibitor of AKT) were used. **B**, mRNA levels of atrial natriuretic peptide (ANP) in indicated groups (n=5). **C** and **D**, Calcineurin activity in the hearts following AB with overexpression or knockdown of S100a9 (n=6). **E** and **F**, NFAT transcriptional activity in the hearts following AB with overexpression or knockdown of S100a9 (n=6). **G** and **H**, mRNA level of calcineurin 1 (RCAN1) in the hearts following AB with overexpression or knockdown of S100a9 (n=6). **I**, Representative Western blots and the statistical results of the protein levels (n=6). Values represent the mean \pm SEM. *P<0.05 vs the matched control group. AB indicates aortic banding; ANP, atrial natriuretic peptide; NF- κ B, nuclear factor- κ B; NFAT, nuclear factor of activated T cells; NRCM, neonatal rat cardiomyocyte; PCNA, proliferating cell nuclear antigen; PLC γ , phospholipase C- γ ; P-PLC γ , phospho-PLC γ ; RCAN1, regulator of calcineurin 1; and S100a8/9, S100 calcium binding protein a8/9.

attenuated AB-induced hypertrophic response and forced expression of S100a9 with AAV-mediated gene transfer aggravated pressure overload-induced cardiac hypertrophy in mice. Investigations of the underlying mechanisms demonstrated that FGF23 is upregulated in cardiac tissues after S100a9 overexpression, which leads to an activation of calcineurin/NFATc3 signaling

pathway, promoting the development of cardiac hypertrophy in mice. Our findings suggested that S100a8/9 was instrumental for the development of pressure overload-induced cardiac hypertrophy.

Here, we observed that the mRNA and protein expression levels of S100a8/9 were significantly upregulated in mice subjected to pressure overload. The

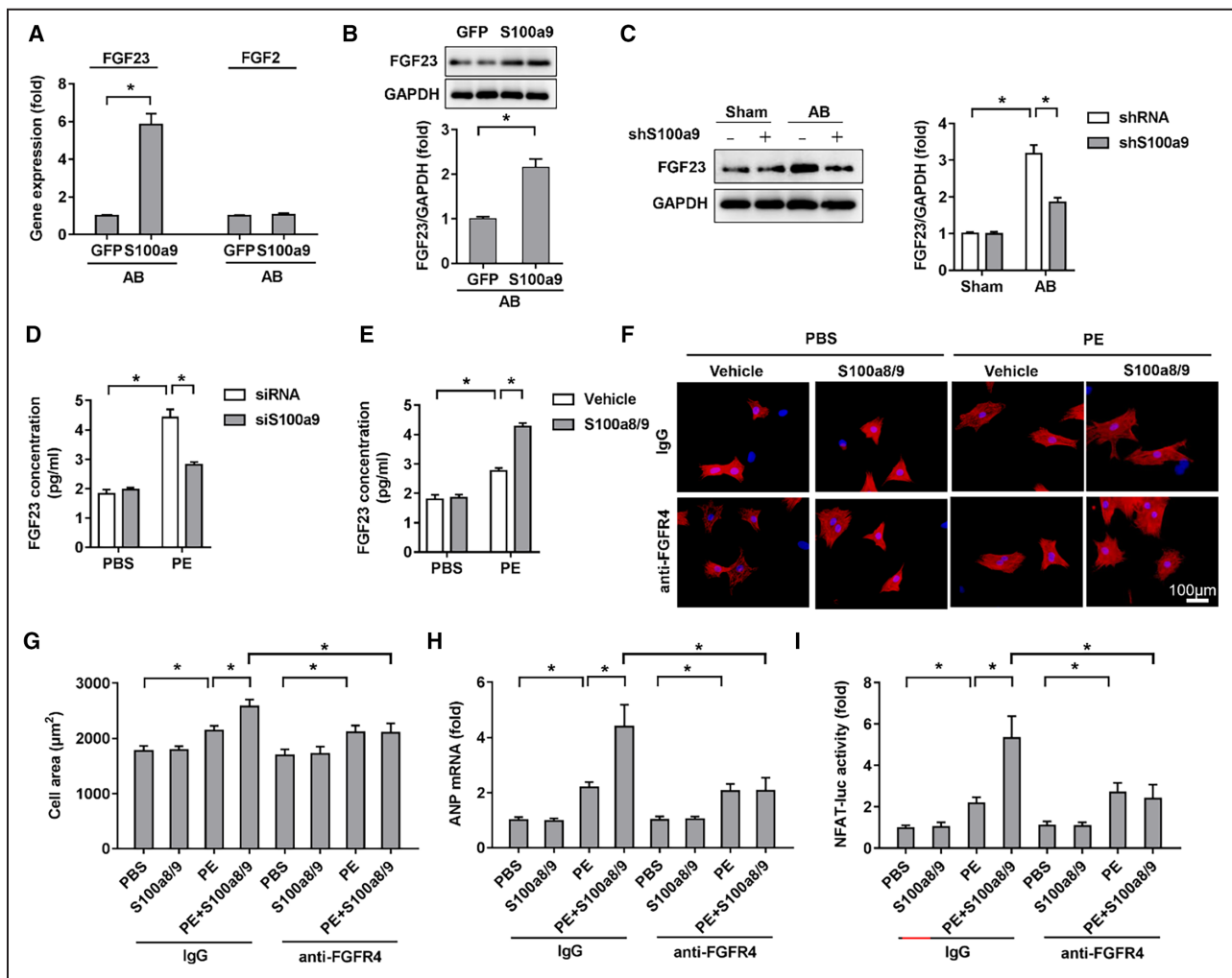


Figure 6. Mice with S100a9 overexpression exhibited increased cardiac expression of FGF23.

A, FGF23 and FGF2 mRNA levels in S100a9-overexpressed and control groups after AB surgery (n=5). **B** and **C**, Representative Western blots and quantitative results of FGF23 in S100a9-overexpression or knockdown mice after AB surgery (n=6). **D** through **E**, FGF23 concentration in phenylephrine-treated NRCMs after simulated by recombinant S100a8/9 or siS100a9 (n=6). **F** and **G**, Representative α -actinin staining and cell area in NRCMs treated with anti-FGFR4 or not (n=5). **H**, mRNA levels of ANP in NRCMs of indicated groups (n=5). **I**, NFAT transcriptional activity in NRCMs of indicated groups (n=5). Values represent the mean \pm SEM. * P <0.05 vs the matched control group. AB indicates aortic banding; ANP, atrial natriuretic peptide; FGF23, fibroblast growth factor 23; FGFR4, FGF receptor 4; IgG, immunoglobulin G; NFAT-luc, nuclear factor of activated T cells-luciferase; NRCM, neonatal rat cardiomyocyte; and S100a8/9, S100 calcium binding protein a8/9.

similar trend of S100a8/9 was also observed in acute coronary syndromes,²⁵ endotoxin-induced cardiomyopathy,¹⁴ and doxorubicin-induced cardiac injury.¹² However, inconsistent with these findings, Yang et al. found that S100a9 was upregulated by 6-fold during regression of cardiac hypertrophy with the use of gene array.²⁶ The different expression of S100a8/9 might be explained by the different animal models. The upregulated expression of S100a8/9 during the hypertrophic response suggested a critical role for S100a8/9 in the onset and development of cardiac hypertrophy. Interestingly, we found that cardiac-specific overexpression of S100a9 aggravated cardiac hypertrophy, and conversely, cardiac-specific ablation of S100a9

attenuated this pathological hypertrophic response in mice. The in vitro experiments also confirmed this prohypertrophic effect of S100a8/9. The maladaptive role in cardiovascular diseases has been confirmed in several teams with different animal models.^{14-15,23} However, there sounded an opposite voice that S100a8/9 mediated the cardio-protection of hypertrophic preconditioning on cardiomyocyte hypertrophy.²⁷ These incompatible results may be attributed to the different interventions and different time point of this disease model.

Plasma FGF23 and S100a8/9 were closely associated with cardiovascular mortality in patients with end-stage renal disease, implying a potential

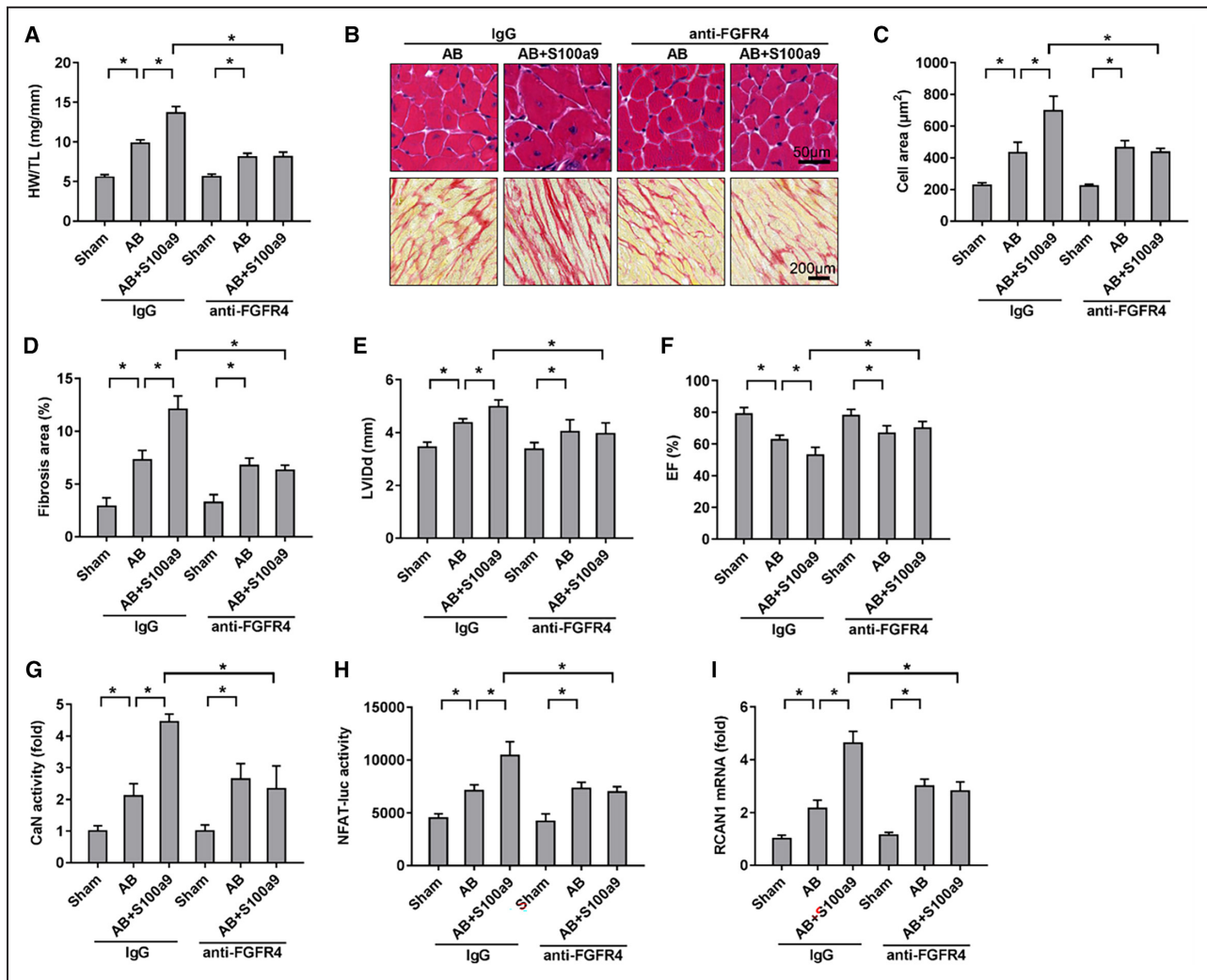


Figure 7. FGFR4 blocking abolished the prohypertrophic effect of S100a8/9 overexpression in response to pressure overload.

A, Statistical results of the HW/TL of mice injected with an FGFR4 blocking antibody (anti-FGFR4) ($n=8-10$). **B**, Hematoxylin–eosin and picrosirius red staining of hearts with anti-FGFR4 or not ($n=4-5$). **C**, The cross-sectional areas of myocytes ($n=4-5$). **D**, Statistical results of the fibrosis areas ($n=4-5$). **E** and **F**, LVIDd and EF of mice with anti-FGFR4 or not ($n=8-10$). **G** through **I**, Calcineurin activity, NFAT transcriptional activity, and RCAN1 mRNA level in hearts with anti-FGFR4 or not ($n=4-5$). Values represent the mean \pm SEM. * $P<0.05$ vs the matched control group. AB indicates aortic banding; EF, ejection fraction; FGFR4, fibroblast growth factor receptor 4; HW, heart weight; IgG, immunoglobulin G; LVIDd, left ventricular internal diastolic diameter; NFAT-luc, nuclear factor of activated T cells-luciferase; RCAN1, regulator of calcineurin 1; S100a8/9, S100 calcium binding protein a8/9; and TL, tibia length.

synergistic effect between S100a8/9 and FGF23.^{28,29}

Our previous study demonstrated that global overexpression of S100A12 (S100a8/9 homolog) resulted in the augmented expression of FGF23 in cardiac tissues.¹⁵ In the present study, elevated FGF23 expression was also observed in mice with transgenic expression of S100a8/9 after pressure overload. The critical role of FGF23 in S100a8/9-induced hypertrophic response was later confirmed by a study indicating the use of FGFR4 antibody could directly abolish the prohypertrophic effect of FGF23 in mice subjected to pressure overload, which was in line with a previous study indicating that the FGFR4 antibody

could attenuate chronic kidney disease-induced cardiac dysfunction.²¹

FGF23 can activate FGFR4 in cardiac myocytes, which led to the phosphorylation of PLC γ .²¹ The calcineurin/NFAT cascade is a critical downstream target of activated PLC γ .³⁰ Here, we also found that S100a8/9 overexpression enhanced the calcineurin/NFAT expression and activities in hypertrophic mice, whereas S100a8/9 deficiency significantly limited the expression and activities of calcineurin/NFAT. However, the heightened calcineurin/NFAT activity and increased expression of RCAN1 in S100a9-overexpressing mice were also suppressed by using FGFR4 blocking

antibody, which is a crucial target that can be directly activated by FGF23 in the process of cardiac hypertrophy. Furthermore, *in vitro* studies have confirmed that anti-FGFR4 nullified the potentiation of NFAT transcriptional activity induced by S100a8/9 treatment. As a result, we can deduce that FGF23 activate calcineurin/NFAT by interacting with FGFR4, thereby triggering the subsequent prohypertrophic responses. Similarly, Bogdanova et al have discovered that calcineurin/NFAT hypertrophic signaling pathway is implicated in myocardial remodeling amid arterial hypertension, potentially mediated by FGF23.³¹ Furthermore, inhibition of PLC γ /calcineurin/NFAT signaling pathway abrogated the prohypertrophic effect of S100a8/9. Our findings were consistent with several studies that suppression of PLC γ /calcineurin/NFAT could attenuate or prevent pathological cardiac hypertrophy in mice.^{32,33}

There comes another question about which factor was responsible for the elevation of FGF23 in S100a8/9-mediated hypertrophic response. The data from our and other laboratories found that FGF23 is induced by several inflammatory signals.^{34,35} However, S100a8/9-caused hypertrophic response was not prevented by an NF- κ B inhibitor in the present study. Unexpectedly but interestingly, we observed enhanced ROS production in S100a8/9-treated cells after PE treatment. Furthermore, NAC prevented S100a8/9-induced hypertrophic response and FGF23 production in cells, implying that S100a8/9-induced FGF23 production might rely on the production of ROS during hypertrophic response.

CONCLUSIONS

In conclusion, our study reported an exacerbated role of S100a8/9 in pressure overload-induced cardiac hypertrophy and dysfunction via increased expression of FGF23. Our findings provide therapeutic targets and strategies for the treatment of cardiac hypertrophy and heart failure.

ARTICLE INFORMATION

Received August 30, 2022; accepted April 4, 2024.

Affiliations

Department of Cardiology, Renmin Hospital of Wuhan University, Wuhan, China (Y.-P.Y., Z.-Y.S., T.T., S.-C.X., C.-Y.K., X.-F.Z., L.Y.); Hubei Key Laboratory of Metabolic and Chronic Diseases, Wuhan, China (Y.-P.Y., Z.-Y.S., T.T., S.-C.X., C.-Y.K., X.-F.Z., L.Y.); and Division of Cardiology, Department of Internal Medicine, University of Michigan, Ann Arbor, MI (M.A.H.B.).

Sources of Funding

This work was supported by grants from the National Natural Science Foundation of China (No. 81870299), Guiding Fund of Renmin Hospital of Wuhan University (No. RMYD2018M39), The Open Project of Hubei Key Laboratory (No. 2023KFZZ027).

Disclosures

None.

Supplemental Material

Figures S1–S3

REFERENCES

1. Frey N, Katus HA, Olson EN, Hill JA. Hypertrophy of the heart: a new therapeutic target? *Circulation*. 2004;109:1580–1589. doi: [10.1161/01.CIR.0000120390.68287.BB](https://doi.org/10.1161/01.CIR.0000120390.68287.BB)
2. Luo Y, Jiang N, May HI, Luo X, Ferdous A, Schiattarella GG, Chen G, Li Q, Li C, Rothermel BA, et al. Cooperative binding of ETS2 and NFAT links Erk1/2 and calcineurin signaling in the pathogenesis of cardiac hypertrophy. *Circulation*. 2021;144:34–51. doi: [10.1161/CIRCULATIONAHA.120.052384](https://doi.org/10.1161/CIRCULATIONAHA.120.052384)
3. Zhang Y, Su SA, Li W, Ma Y, Shen J, Wang Y, Shen Y, Chen J, Ji Y, Xie Y, et al. Piezo1-mediated mechanotransduction promotes cardiac hypertrophy by impairing calcium homeostasis to activate calpain/calcineurin signaling. *Hypertension*. 2021;78:647–660. doi: [10.1161/HYPERTENSIONAHA.121.17177](https://doi.org/10.1161/HYPERTENSIONAHA.121.17177)
4. Pan B, Li J, Parajuli N, Tian Z, Wu P, Lewno MT, Zou J, Wang W, Bedford L, Mayer RJ, et al. The calcineurin-TFEB-p62 pathway mediates the activation of cardiac macroautophagy by proteasomal malfunction. *Circ Res*. 2020;127:502–518. doi: [10.1161/CIRCRESAHA.119.316007](https://doi.org/10.1161/CIRCRESAHA.119.316007)
5. Fiedler B, Wollert KC. Targeting calcineurin and associated pathways in cardiac hypertrophy and failure. *Expert Opin Ther Targets*. 2005;9:963–973. doi: [10.1517/14728222.9.5.963](https://doi.org/10.1517/14728222.9.5.963)
6. Li X, Li J, Martinez EC, Froese A, Passariello CL, Henshaw K, Rusconi F, Li Y, Yu Q, Thakur H, et al. Calcineurin Abeta-specific anchoring confers isoform-specific compartmentation and function in pathological cardiac myocyte hypertrophy. *Circulation*. 2020;142:948–962. doi: [10.1161/CIRCULATIONAHA.119.044893](https://doi.org/10.1161/CIRCULATIONAHA.119.044893)
7. Martinez-Martinez S, Lozano-Vidal N, Lopez-Maderuelo MD, Jimenez-Borreguero LJ, Armesilla AL, Redondo JM. Cardiomyocyte calcineurin is required for the onset and progression of cardiac hypertrophy and fibrosis in adult mice. *FEBS J*. 2019;286:46–65. doi: [10.1111/febs.14718](https://doi.org/10.1111/febs.14718)
8. Leinwand LA. Calcineurin inhibition and cardiac hypertrophy: a matter of balance. *Proc Natl Acad Sci USA*. 2001;98:2947–2949. doi: [10.1073/pnas.051033698](https://doi.org/10.1073/pnas.051033698)
9. Quoc QL, Choi Y, Thi BT, Yang EM, Shin YS, Park HS. S100A9 in adult asthmatic patients: a biomarker for neutrophilic asthma. *Exp Mol Med*. 2021;53:1170–1179. doi: [10.1038/s12276-021-00652-5](https://doi.org/10.1038/s12276-021-00652-5)
10. Cotoi OS, Duner P, Ko N, Hedblad B, Nilsson J, Bjorkbacka H, Schiopu A. Plasma S100A8/A9 correlates with blood neutrophil counts, traditional risk factors, and cardiovascular disease in middle-aged healthy individuals. *Arterioscler Thromb Vasc Biol*. 2014;34:202–210. doi: [10.1161/ATVBAHA.113.302432](https://doi.org/10.1161/ATVBAHA.113.302432)
11. Boteanu RM, Suica VI, Uyy E, Ivan L, Cerveanu-Hogas A, Mares RG, Simionescu M, Schiopu A, Antohe F. Short-term blockade of pro-inflammatory alarmin S100A9 favorably modulates left ventricle proteome and related signaling pathways involved in post-myocardial infarction recovery. *Int J Mol Sci*. 2022;23:5289. doi: [10.3390/ijms23095289](https://doi.org/10.3390/ijms23095289)
12. Pei XM, Tam BT, Sin TK, Wang FF, Yung BY, Chan LW, Wong CS, Ying M, Lai CW, Siu PM. S100A8 and S100A9 are associated with doxorubicin-induced cardiotoxicity in the heart of diabetic mice. *Front Physiol*. 2016;7:334. doi: [10.3389/fphys.2016.00334](https://doi.org/10.3389/fphys.2016.00334)
13. Muller I, Vogl T, Pappritz K, Miteva K, Savvatis K, Rohde D, Most P, Lassner D, Pieske B, Kuhl U, et al. Pathogenic role of the damage-associated molecular patterns S100A8 and S100A9 in coxsackievirus B3-induced myocarditis. *Circ Heart Fail*. 2017;10:e004125. doi: [10.1161/CIRCHEARTFAILURE.117.004125](https://doi.org/10.1161/CIRCHEARTFAILURE.117.004125)
14. Boyd JH, Kan B, Roberts H, Wang Y, Walley KR. S100A8 and S100A9 mediate endotoxin-induced cardiomyocyte dysfunction via the receptor for advanced glycation end products. *Circ Res*. 2008;102:1239–1246. doi: [10.1161/CIRCRESAHA.107.167544](https://doi.org/10.1161/CIRCRESAHA.107.167544)
15. Yan L, Mathew L, Chellan B, Gardner B, Earley J, Puri TS, Hofmann Bowman MA. S100/Calgranulin-mediated inflammation accelerates left ventricular hypertrophy and aortic valve sclerosis in chronic kidney disease in a receptor for advanced glycation end products-dependent manner. *Arterioscler Thromb Vasc Biol*. 2014;34:1399–1411. doi: [10.1161/ATVBAHA.114.303508](https://doi.org/10.1161/ATVBAHA.114.303508)
16. Zhang X, Hu C, Kong CY, Song P, Wu HM, Xu SC, Yuan YP, Deng W, Ma ZG, Tang QZ. FNDC5 alleviates oxidative stress and cardiomyocyte

- apoptosis in doxorubicin-induced cardiotoxicity via activating AKT. *Cell Death Differ*. 2020;27:540–555. doi: [10.1038/s41418-019-0372-z](https://doi.org/10.1038/s41418-019-0372-z)
17. Ma ZG, Yuan YP, Xu SC, Wei WY, Xu CR, Zhang X, Wu QQ, Liao HH, Ni J, Tang QZ. CTRP3 attenuates cardiac dysfunction, inflammation, oxidative stress and cell death in diabetic cardiomyopathy in rats. *Diabetologia*. 2017;60:1126–1137. doi: [10.1007/s00125-017-4232-4](https://doi.org/10.1007/s00125-017-4232-4)
 18. Yuan Y, Yan L, Wu QQ, Zhou H, Jin YG, Bian ZY, Deng W, Yang Z, Shen DF, Zeng XF, et al. Mnk1 (mitogen-activated protein kinase-interacting kinase 1) deficiency aggravates cardiac remodeling in mice. *Hypertension*. 2016;68:1393–1399. doi: [10.1161/HYPERTENSIONAHA.116.07906](https://doi.org/10.1161/HYPERTENSIONAHA.116.07906)
 19. Zhou H, Li N, Yuan Y, Jin YG, Wu Q, Yan L, Bian ZY, Deng W, Shen DF, Li H, et al. Leukocyte immunoglobulin-like receptor B4 protects against cardiac hypertrophy via SHP-2-dependent inhibition of the NF-kappaB pathway. *J Mol Med (Berl)*. 2020;98:691–705. doi: [10.1007/s00109-020-01896-w](https://doi.org/10.1007/s00109-020-01896-w)
 20. Ma ZG, Yuan YP, Zhang X, Xu SC, Kong CY, Song P, Li N, Tang QZ. C1q-tumour necrosis factor-related protein-3 exacerbates cardiac hypertrophy in mice. *Cardiovasc Res*. 2019;115:1067–1077. doi: [10.1093/cvr/cvy279](https://doi.org/10.1093/cvr/cvy279)
 21. Grabner A, Amaral AP, Schramm K, Singh S, Sloan A, Yanucil C, Li J, Shehadeh LA, Hare JM, David V, et al. Activation of cardiac fibroblast growth factor receptor 4 causes left ventricular hypertrophy. *Cell Metab*. 2015;22:1020–1032. doi: [10.1016/j.cmet.2015.09.002](https://doi.org/10.1016/j.cmet.2015.09.002)
 22. Manitz MP, Horst B, Seeliger S, Strey A, Skryabin BV, Gunzer M, Frings W, Schonlau F, Roth J, Sorg C, et al. Loss of S100A9 (MRP14) results in reduced interleukin-8-induced CD11b surface expression, a polarized microfilament system, and diminished responsiveness to chemo-attractants in vitro. *Mol Cell Biol*. 2003;23:1034–1043. doi: [10.1128/MCB.23.3.1034-1043.2003](https://doi.org/10.1128/MCB.23.3.1034-1043.2003)
 23. Li Y, Chen B, Yang X, Zhang C, Jiao Y, Li P, Liu Y, Li Z, Qiao B, Bond LW, et al. S100a8/a9 signaling causes mitochondrial dysfunction and cardiomyocyte death in response to ischemic/reperfusion injury. *Circulation*. 2019;140:751–764. doi: [10.1161/CIRCULATIONAHA.118.039262](https://doi.org/10.1161/CIRCULATIONAHA.118.039262)
 24. Yang J, Rothermel B, Vega RB, Frey N, McKinsey TA, Olson EN, Bassel-Duby R, Williams RS. Independent signals control expression of the calcineurin inhibitory proteins MCIP1 and MCIP2 in striated muscles. *Circ Res*. 2000;87:E61–E68. doi: [10.1161/01.RES.87.12.e61](https://doi.org/10.1161/01.RES.87.12.e61)
 25. Altwegg LA, Neidhart M, Hersberger M, Muller S, Eberli FR, Corti R, Roffi M, Sutsch G, Gay S, von Eckardstein A, et al. Myeloid-related protein 8/14 complex is released by monocytes and granulocytes at the site of coronary occlusion: a novel, early, and sensitive marker of acute coronary syndromes. *Eur Heart J*. 2007;28:941–948. doi: [10.1093/eurheartj/ehm078](https://doi.org/10.1093/eurheartj/ehm078)
 26. Yang DK, Choi BY, Lee YH, Kim YG, Cho MC, Hong SE, Kim DH, Hajjar RJ, Park WJ. Gene profiling during regression of pressure overload-induced cardiac hypertrophy. *Physiol Genomics*. 2007;30:1–7. doi: [10.1152/physiolgenomics.00246.2006](https://doi.org/10.1152/physiolgenomics.00246.2006)
 27. Wei X, Wu B, Zhao J, Zeng Z, Xuan W, Cao S, Huang X, Asakura M, Xu D, Bin J, et al. Myocardial hypertrophic preconditioning attenuates cardiomyocyte hypertrophy and slows progression to heart failure through upregulation of S100A8/A9. *Circulation*. 2015;131(1506–1517):1517.
 28. Shiotsu Y, Mori Y, Nishimura M, Sakoda C, Tokoro T, Hatta T, Maki N, Iida K, Iwamoto N, Ono T, et al. Plasma S100A12 level is associated with cardiovascular disease in hemodialysis patients. *Clin J Am Soc Nephrol*. 2011;6:718–723. doi: [10.2215/CJN.08310910](https://doi.org/10.2215/CJN.08310910)
 29. Faul C, Amaral AP, Oskouei B, Hu MC, Sloan A, Isakova T, Gutierrez OM, Aguilon-Prada R, Lincoln J, Hare JM, et al. FGF23 induces left ventricular hypertrophy. *J Clin Invest*. 2011;121:4393–4408. doi: [10.1172/JCI46122](https://doi.org/10.1172/JCI46122)
 30. Crabtree GR, Olson EN. NFAT signaling: choreographing the social lives of cells. *Cell*. 2002;109(suppl):S67–S79. doi: [10.1016/S0092-8674\(02\)00699-2](https://doi.org/10.1016/S0092-8674(02)00699-2)
 31. Bogdanova E, Beresneva O, Galkina O, Zubina I, Ivanova G, Parastayeva M, Semenova N, Dobronravov V. Myocardial hypertrophy and fibrosis are associated with cardiomyocyte beta-catenin and TRPC6/calci-neurin/NFAT signaling in spontaneously hypertensive rats with 5/6 nephrectomy. *Int J Mol Sci*. 2021;22:4645. doi: [10.3390/ijms22094645](https://doi.org/10.3390/ijms22094645)
 32. Han X, Cai C, Xiao Z, Quarles LD. FGF23 induced left ventricular hypertrophy mediated by FGFR4 signaling in the myocardium is attenuated by soluble klotho in mice. *J Mol Cell Cardiol*. 2020;138:66–74. doi: [10.1016/j.yjmcc.2019.11.149](https://doi.org/10.1016/j.yjmcc.2019.11.149)
 33. Remes A, Wagner AH, Schmiedel N, Heckmann M, Ruf T, Ding L, Jungmann A, Senger F, Katus HA, Ullrich ND, et al. AAV-mediated expression of NFAT decoy oligonucleotides protects from cardiac hypertrophy and heart failure. *Basic Res Cardiol*. 2021;116:38. doi: [10.1007/s00395-021-00880-w](https://doi.org/10.1007/s00395-021-00880-w)
 34. Yan L, Bowman MA. Chronic sustained inflammation links to left ventricular hypertrophy and aortic valve sclerosis: a new link between S100/RAGE and FGF23. *Inflamm Cell Signal*. 2014;1:e279.
 35. Poss J, Mahfoud F, Seiler S, Heine GH, Fliser D, Bohm M, Link A. FGF-23 is associated with increased disease severity and early mortality in cardiogenic shock. *Eur Heart J Acute Cardiovasc Care*. 2013;2:211–218. doi: [10.1177/2048872613494025](https://doi.org/10.1177/2048872613494025)